

## XPS and $\mu$ -Raman study of nanosecond-laser processing of poly(dimethylsiloxane) (PDMS)



S. Armyanov<sup>a,\*</sup>, N.E. Stankova<sup>b</sup>, P.A. Atanasov<sup>b</sup>, E. Valova<sup>a</sup>, K. Kolev<sup>a</sup>, J. Georgieva<sup>a</sup>, O. Steenhaut<sup>c</sup>, K. Baert<sup>c</sup>, A. Hubin<sup>c</sup>

<sup>a</sup>Rostislav Kaischew Institute of Physical Chemistry, Bulgarian Academy of Sciences, Acad. G. Bonchev Str., Block 11, Sofia 1113, Bulgaria

<sup>b</sup>Institute of Electronics, Bulgarian Academy of Sciences, 72 Tsarigradsko Shose, Sofia 1784, Bulgaria

<sup>c</sup>Vrije Universiteit Brussels, Faculty of Engineering, Research Group, SURF "Electrochemical and Surface Engineering", Belgium

### ARTICLE INFO

#### Article history:

Received 16 July 2015

Accepted 31 July 2015

#### Keywords:

Poly(dimethylsiloxane) (PDMS)

Nanosecond Nd:YAG laser

$\mu$ -Raman spectroscopy

XPS

### ABSTRACT

Data about the chemical status of poly(dimethylsiloxane) (PDMS) after nanosecond Q-switched Nd:YAG laser treatment with near infrared, visible and ultraviolet radiation are presented. The  $\mu$ -Raman spectroscopy analyses reveal as irradiation result a new sharp peak of crystalline silicon. In addition, broad bands appear assigned to D band of amorphous carbon and G band of microcrystalline and polycrystalline graphite. The  $\mu$ -Raman spectra are variable taken in different inspected points in the trenches formed by laser treatment. The XPS surface survey spectra indicate the constituent elements of PDMS: carbon, oxygen and silicon. The spectra of detail XPS scans illustrate the influence of the laser treatment. The position of Si 2p peaks of the treated samples is close to the value of non-treated except that irradiated by 1064 nm 66 pulses, which is shifted by 0.9 eV. Accordingly, a shift by 0.4 eV is noticed of the O 1s peak, which reflects again a stronger oxidation of silicon. The curve fitting of Si 2p and O 1s peaks after this particular laser treatment shows the degree of conversion of organic to inorganic silicon that takes place during the irradiation.

© 2015 Elsevier B.V. All rights reserved.

### 1. Introduction

Poly(dimethylsiloxane) (PDMS) is optically transparent, durable, non-fluorescent, biocompatible, chemically inert and nontoxic. Only strong acids or strong bases are capable to depolymerize the siloxane chain. As a result, the PDMS polymers are not very susceptible to oxidation or thermal degradation and they can be sterilized by heat. Besides its well-known superior elasticity and flexibility in mechanical applications, PDMS has become a popular choice for biological studies because of its non-toxicity to cells and high permeability to gases [1,2]. Thus PDMS is an important material for the development of microelectromechanical systems (MEMS) or long-term, biocompatible implants [3].

After polymerization solid PDMS samples will present an external hydrophobic surface [4]. Thus, it is difficult to be wetted by polar solvents (such as water). Many of the applications of PDMS are connected with the modification of the PDMS surface in order to change the morphology and chemical composition. The most used method is a plasma oxidation (atmospheric air plasma,

oxygen and argon plasma) for altering the chemical properties of the surface, i.e. creation of superficial silanol (SiOH) groups [5]. A number of investigations show that after a certain amount of time following the plasma treatment, recovery of the surface's hydrophobicity is inevitable, regardless of whether the surrounding medium is vacuum, air, or water [6]. The temporal evolution of the contact angles between the deionized water and PDMS treated with O<sub>2</sub> plasma could be seen in Fig. 3 of Ref. [7].

An alternative method for modifications of PDMS is the laser treatment. The ablation by laser pulses is always a mixture of photochemical and photothermal reactions, where the ratio between them is a function of the polymer properties and the laser parameters [8]. The changes of the irradiated parts of the surface depend on the type of fluence source: UV-generated Nd:YAG laser or KrF-excimer laser [9,10]. Several common features and some specific differences can be summarized. (i) At similar wavelength, energy density, number of subsequent pulses and repetition rate, the ablation depths are larger in case of UV-generated Nd:YAG laser. (ii) At lower pulse numbers swelling of PDMS is observed only when excimer laser is used. (iii) The ablation depth increases with repetition rate when the excimer laser is applied at the same energy density and pulse number. (iv) An increase of Si in the EDS

\* Corresponding author. Tel.: +359 878 870037; fax: +359 2 971 2688.

E-mail address: [armyanov@ipc.bas.bg](mailto:armyanov@ipc.bas.bg) (S. Armyanov).

spectra was observed acquired on PDMS irradiated with Nd:YAG laser in comparison with those on native PDMS [10]. Laser treatment is used in order to facilitate selective metallization of the areas activated in this way [11–15].

After irradiation of PDMS with a Nd:YAG laser, the  $\mu$ -Raman spectrum presents a new peak at  $516\text{ cm}^{-1}$ , which can be assigned to nanocrystalline silicon [9,10,13,14]. The sharp peak between  $512$  and  $518\text{ cm}^{-1}$  appears also in the case of processing with visible light (VIS) of nanosecond Nd:YAG laser ( $532\text{ nm}$ ) and femtosecond laser ( $527\text{ nm}$ ), which is the first observation of c-Si formation by irradiation of PDMS with VIS femtosecond pulses [15]. This can be ascribed to mono and/or polycrystalline or only to monocrystalline silicon (c-Si) [16]. Its intensity increases with the number of the pulses and the laser fluence. Moreover, in the  $\mu$ -Raman spectra broad bands appear between  $1320\text{ cm}^{-1}$  and  $1603\text{ cm}^{-1}$  depending on the experimental conditions, which can be assigned to D band of the amorphous carbon and the G band of polycrystalline and microcrystalline graphite, respectively [9,10,14,15].

Investigations with X-ray photoelectron spectroscopy (XPS) of the modification of PDMS films induced by UV irradiation are reported [17]. It is obtained that the binding energies (BEs) of the Si 2p and O 1s increase and reach the values corresponding to  $\text{SiO}_2$ . After spin-coated films of PDMS exposure to microwave oxygen plasma XPS data show, that a significant proportion of the oxidized layer contained silicon bonded to 3 or 4 oxygen atoms ( $\text{SiO}_x$ ) [18]. The degree of conversion of organic to inorganic silicon ( $\text{SiO}_x$ ) increased with increasing microwave plasma dose. A similar result is obtained for samples exposed to corona discharges [19].

We did not find any XPS data about the chemical transformations after laser treatment of PDMS. Nevertheless there is information that the PDMS surface layer after other types of irradiation becomes enriched in oxygen and depleted in carbon [20,21,17]. It is supposed also, that the methyl group  $\text{CH}_3$  could be replaced not only by oxygen, but by hydroxyl group OH also [20,21].

The aim of the present paper is to provide complex data of the chemical status of PDMS after near infrared (NIR), visible (VIS) and ultraviolet (UV) radiation of the nanosecond (ns)-laser treatment. It emphasizes the XPS investigations in conjunction with the additional data taken by SEM and  $\mu$ -Raman spectroscopy analyses.

## 2. Experimental

### 2.1. Material and treatment

PDMS-elastomer sheets (KCC-corporation, South Korea) ( $800\text{ }\mu\text{m}$  thick) are irradiated with basic harmonic ( $\lambda = 1064\text{ nm}$ ), as well as second harmonic (SHG) ( $\lambda = 532\text{ nm}$ ), third harmonic (THG) ( $\lambda = 355\text{ nm}$ ) and fourth harmonic (FHG) ( $\lambda = 266\text{ nm}$ ) of

Q-switched Nd:YAG laser (pulse duration  $\tau = 15\text{ ns}$  and pulse repetition rate of  $10\text{ Hz}$ ) in air at ambient temperature. The samples are mounted on a microcontroller-driven, stepper-motor operated X–Y table. The minimum step size of the translation stage is  $12.7\text{ }\mu\text{m}$ . Laser beam is focused by a lens with  $22\text{ cm}$  focal length. The micro-channels (trenches) are produced in “scanning mode” by simultaneously moving the samples perpendicularly with respect to the laser beam. The number of the consecutive pulses (from 11 to 110) per laser beam spot on the material surface is controlled by the moving speed of the table. Continuous trenches with lengths between  $3$  and  $10\text{ mm}$  and widths between  $50$  and  $500\text{ }\mu\text{m}$ , depending on the laser parameters, are produced. Larger widths are produced especially for the samples prepared for XPS analyses.

### 2.2. Measurements

Different experimental techniques are applied to characterize the native PDMS-elastomer, as well as the irradiated tracks: JEOL JSM-7000F field emission Scanning Electron Microscopy (SEM);  $\mu$ -Raman spectrometry (LabRAM HR Evolution-Horiba Scientific), equipped with  $100\times$  magnification objective and excited by solid state laser source operating at  $\lambda = 532\text{ nm}$ . The  $\mu$ -Raman spectra of the laser treated PDMS surface are acquired from different sections at the bottom of each trench and compared to the Raman signals of the native material.

X-ray Photo electron Spectroscopy (XPS) studies are performed in a PHI model 5600 system equipped with an Omni Focus Lens III using a standard Mg  $K\alpha$  X-ray source at a high voltage of  $15\text{ kV}$ ,  $300\text{ W}$ . The PHI Multipak 9 software is used for data treatment and interpretation.

## 3. Results and discussion

Typical picture of the trench formed after the laser ablation by NIR laser radiation is exposed on Fig. 1. It is clear that the profile of the trench is characterized by extremely developed surface with caves, which can ensure good adhesion of the metal coating deposited on it.

Fig. 2 (a and b) display the  $\mu$ -Raman spectra of the processed by NIR laser pulses as well as non-processed (native) PDMS. One can see that a sharp peak of crystalline silicon (c-Si) adjacent to the peaks of native PDMS is observed as result of laser treatment. Its intensity increases with laser fluence and number of subsequent laser pulses at all applied laser wavelengths. At higher fluence and number of pulses broad bands assigned to the D band of amorphous carbon and the G band of polycrystalline and microcrystalline graphite also appear (Fig. 2a), confirming findings described before [9,10,14,15]. Moreover, spectra variations are

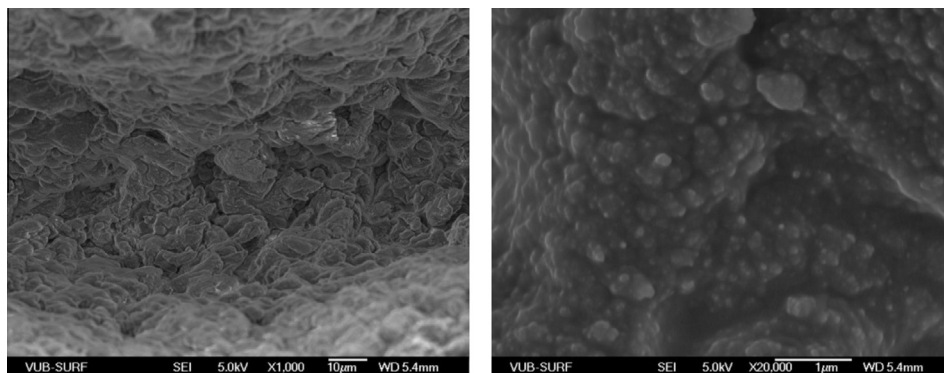
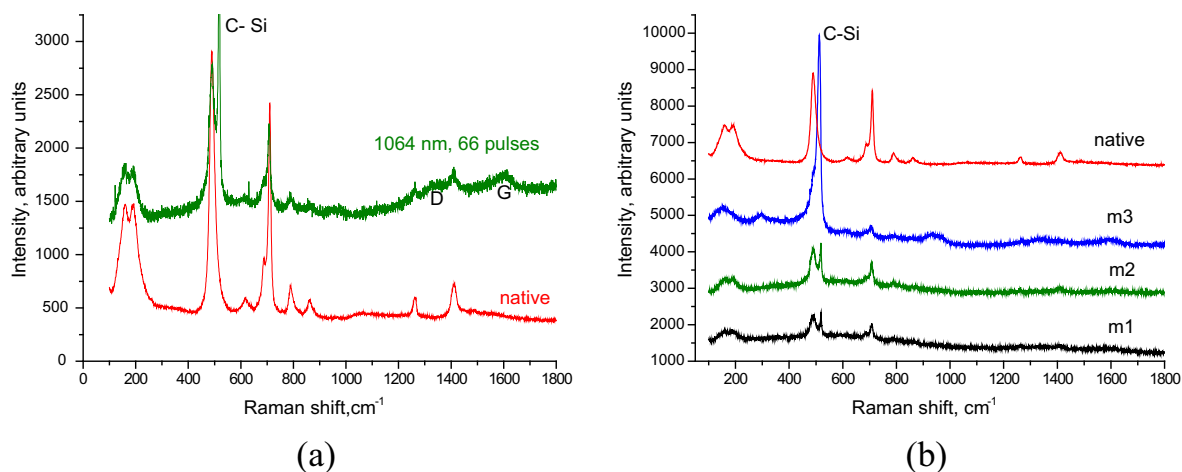


Fig. 1. Tracks produced by nanosecond laser with  $\lambda = 1064\text{ nm}$ , 66 pulses,  $6.4\text{ J cm}^{-2}$ .



**Fig. 2.**  $\mu$ -Raman spectra of native and ns-laser processed PDMS-elastomer. Irradiation with  $\lambda = 1064$  nm and 66 pulses was applied. Laser fluence is  $6.4 \text{ J cm}^{-2}$  (a). For a comparison the spectra in 3 different points (m1, m2, m3) are presented (b).

observed in different points inspected in a trench: Fig. 2b. This can be explained by the inhomogeneity of the laser: “hot spot”. In fact the laser spot has multimode structures.

XPS and  $\mu$ -Raman analyses are conducted about a month after the laser treatment. The surface survey spectra indicate that the deposits contain carbon, oxygen and silicon, i.e., the constituent elements of PDMS. The spectra of detail scans are shown in Fig. 3, where the influence of the laser treatment is illustrated.

As it is well known during the XPS experiments on non-conducting materials a charge compensation technique should be applied. Despite this the exact BEs of spectral peaks in an insulator might be open to question. Since the shift of all lines in a spectrum due to the charging is the same, if the energy of one line can be established on an absolute basis, the rest of the lines can be calibrated with respect to that one. Carbon is often used for calibration because the carbon peak is found on all samples exposed to the environment [22,23]. In our case we adjust C 1s at a binding energy of PDMS 284.38 eV [24,25]. In this way the differences in O 1s and Si 2p positions could be clearly displayed in Fig. 3, whenever they appear.

The symmetry of the hydrocarbon component of the C1s peak presented in Fig. 3a confirms the validity of this assumption. The peak's full width at half maximum (FWHM) however obviously depends on the treatment regime and varies in each case due to geometrical reasons. There is some ablation difference in areas and complicate shape of the trenches, which is the reason for the observed variations in the peak intensity and their FWHM (see Fig. 1).

It is accepted that even following all recommendations uncertainties between the local measurements and published data about BEs could be reduced to “0.1–0.2 eV” [26]. Detailed analysis of the number of factors affecting the accuracy of BE determination one can find in Refs. [26–28]. In this work we will consider the BE changes in Fig. 3(b and c) comparatively to the BE of non-treated (native) PDMS. The reference values for PDMS BE of O 1s and Si 2p [24,25] are given just for information. One can judge about the reproducibility from comparison of the data of two samples after the exposure to same irradiation 355 nm 110 pulses, which are practically coinciding.

The position of Si 2p peaks in Fig. 3b are close to the value of non-irradiated except the sample treated by NIR irradiation 1064 nm 66 pulses, which is shifted by 0.9 eV with respect to the native. This can be caused by the introduction of oxygen as it is shown after plasma treatment in [29]. It will be discussed in details later. One can find a tendency in an increase of the peaks shift due

to the number of pulses: in the case of NIR 1064 nm it is from 101.9 eV for 11 pulses to 102.9 eV for 66 pulses.

The O 1s peaks presented in Fig. 3c are symmetrical. One can notice that at sample treated by irradiation 1064 nm and 66 pulses the peak is shifted by 0.4 eV, which is beyond the possible inaccuracy. This peak position reflects a stronger oxidation of Si. This will be analyzed also later. Again, one can see the effect of the number of pulses for NIR irradiation 1064 nm: from 532.0 eV for 11 pulses to 532.6 eV for 66 pulses.

The O 1s and Si 2p peaks of the sample treated by NIR irradiation 1064 nm and 66 pulses are deconvolved using the mixed Gaussian/Lorentzian function (PHI Multipak 9) in order to assess the oxidation degree of silicon.

The curve fitting of Si 2p peak after this particular laser treatment is presented in Fig. 4 and Table 1. From these data it is clear that during the irradiation oxidation in different degree takes place. For pure silicon (Si) it is claimed a peak at 99.5 eV corresponding to  $\text{Si}(-\text{OH})_x$  could exist [32]. In our case it is hard to identify such a peak neither in Fig. 3b nor in Fig. 4. In the case of PDMS it looks the chemical condition of Si is determined mainly by its position in the polymer chain and during the oxidation process first of all by bonding with oxygen. In other words, one can expect very low influence of H through O on the BE of Si 1s in this case.

The deconvolution of O 1s peak is presented in Fig. 5 and Table 2. For SiOH in as-received pure Si one could see BE of about 530.4 eV in Fig. 5 of Reference [29]. In the case of special treatment of Si in condition of humidity the BE of  $\text{Si}(\text{OH})_x$  is about 1 eV higher. [29], and references therein]. Also for other substances, different from PDMS, it is reported that BE of O 1s for  $\text{SiO}_{1.8}$  is 532.20 eV [33], for  $\text{SiO}_{1.9}$  is 532.6 eV [34]; and for  $\text{SiO}_2$  533.20 eV [35]. All these data make expectable the peak shift to higher values of BE, when the oxidation degree of Si in PDMS is increased. However, it is hard to make exact predictions. From the data shown in Fig. 5 and Table 2 one can see the BE values of the peaks after the deconvolution are close to the mentioned above for oxidation forms of the pure Si. The areas under the three peaks in Fig. 4 and Table 1 are of the same order as the respective three peaks in Fig. 5 and Table 2.

The silicon–oxygen–silicon linkage in silicones is similar to the linkage in quartz and glass. Laser radiation can't break Si–O bonding but can split Si from carbon. Photodecomposition of PDMS produces volatile carbonaceous cycle, thus being the reason for carbon loss observed by quantitative XPS and EDS after treatment. The remaining Si is bonded with atmospheric oxygen to produce an enrichment in non-stoichiometric oxygen deficient  $\text{SiO}_2$ . The

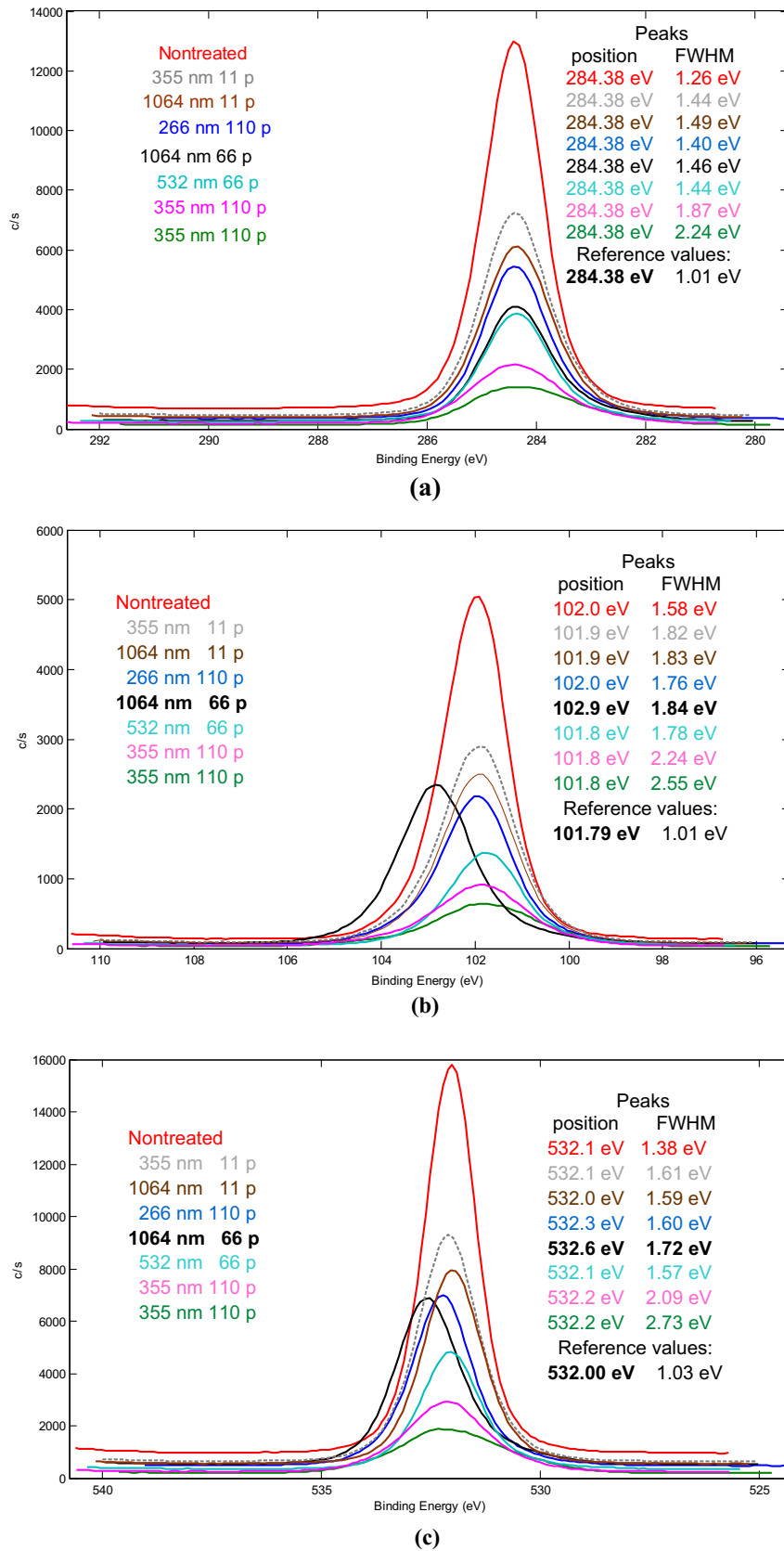


**Fig. 3.** Comparisons of XPS of PDMS treated by ns laser radiation with different wave length ( $\lambda$ ) and pulses number ( $p$ ). All spectra are after shifting C1s to 284.38 eV. The reference values are from [24,25]: (a) C1s; (b) Si 2p; (c) O1s.

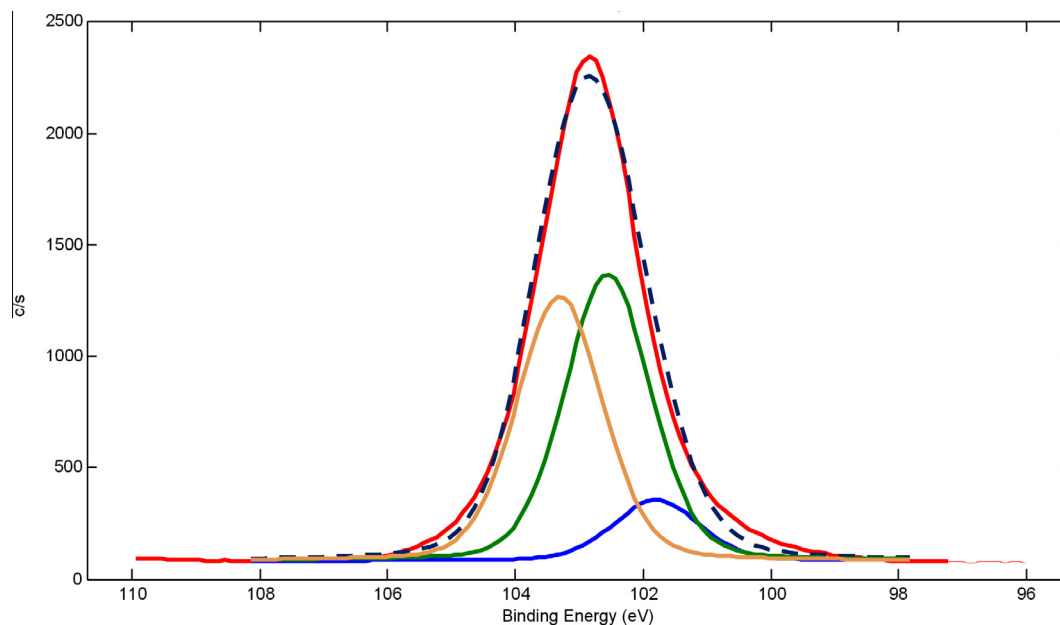


**Fig. 4.** Curve fitting of XPS spectra of Si 2p for 1064 nm 66 pulses 6.5 J/cm<sup>2</sup>. The dashed line is the fitting curve. Blue line Si(-O)<sub>2</sub> 101.8 eV; green line Si(-O)<sub>3</sub> 102.6 eV; orange line Si(-O)<sub>4</sub> 103.3 eV. The areas under the curves are as follows: Si(-O)<sub>2</sub> 10.0%, Si(-O)<sub>3</sub> 46.8%, Si(-O)<sub>4</sub> 43.2% – Table 1. (For interpretation of the references to colour in this figure legend, the reader is referred to the web version of this article.)

**Table 1**  
Silicon chemical environments and the corresponding Si 2p (see also [24,25,29–31]).

Structure			
Abbreviation	Si(-O) <sub>2</sub>	Si(-O) <sub>3</sub>	Si(-O) <sub>4</sub>
Experimental BE (eV)	101.8	102.6	103.3
Reference BE (eV)/	101.79	102.67	103.3
Source	PDMS [24,25]	[30]	SiO <sub>2</sub> [31]
Calculated from fitting in Fig. 4 (%)	10.0	46.8	43.2

**Table 2**  
Oxygen chemical environments and the corresponding O 1s BE.

Structure				
Abbreviation	Si(-OH)	Si(-O) <sub>2</sub>	Si(-O) <sub>3</sub>	Si(-O) <sub>4</sub>
Experimental BE (eV)	530.6	531.6	532.4	533.0
Calculated from fitting in Fig. 5 (%)	4.0	14.4	44.6	36.9

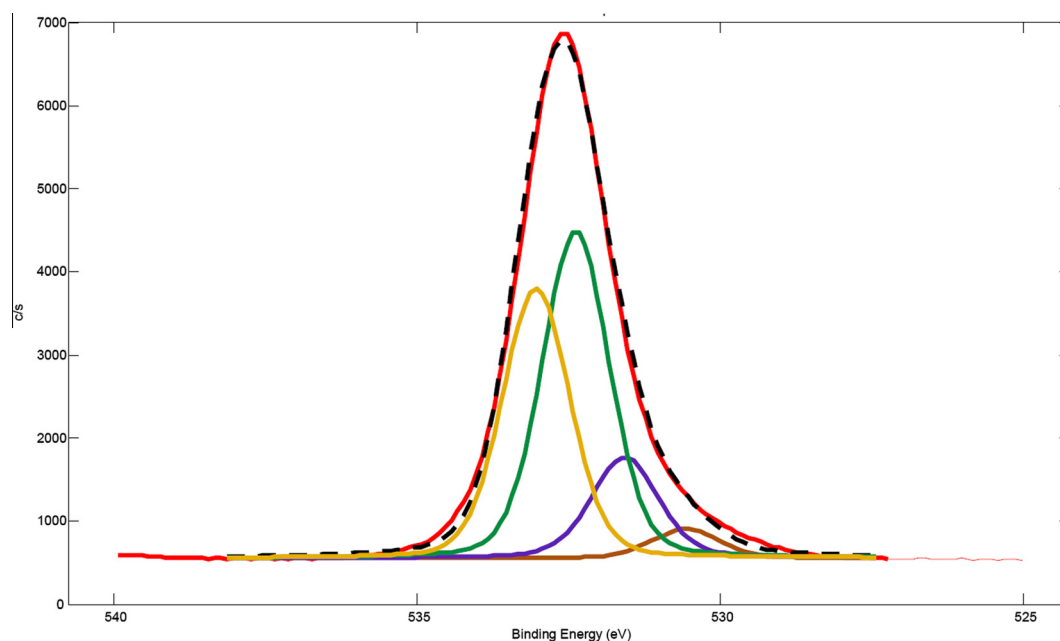


**Fig. 5.** Curve fitting of XPS spectra of O 1s for 1064 nm 66 pulses 6.5 J/cm<sup>2</sup>. The original peak is displayed by a red line, the dashed line is the fitting curve. The areas under the curves are as follows: dark orange (Si(-OH)) 4%, purple (Si(-O)<sub>2</sub>) 14.4%, green (Si(-O)<sub>3</sub>) 44.6%, orange (Si(-O)<sub>4</sub>) 36.9% – Table 2. (For interpretation of the references to colour in this figure legend, the reader is referred to the web version of this article.)

reason to observe a noticeable silicon oxidation only in one case could be a possible recovering of the surface after the laser ablation during one month similar to the development after plasma treatment.

It is interesting now to comment the comparison between the  $\mu$ -Raman spectra and XPS data. One should keep in mind the difference in the sampling depth wherefrom the information is coming in these spectroscopic methods. The difference of this value for XPS and  $\mu$ -Raman is about three orders of magnitude ( $10^3$ ): nanometers and micrometers, respectively. This is making very different the sampling volume also. It could not be surprising to identify crystalline Si inside the layer affected by laser ablation and oxides on the top of this area. The presence of OH groups on the surface is responsible for hydrophilic behavior of laser treated areas being one of the factors enabling electroless metallization.

#### 4. Conclusion

After the ns-laser treatment of medical grade PDMS in the  $\mu$ -Raman spectra a distinct peak of crystalline silicon (c-Si) is displayed, whose intensity increases with laser fluence and number of subsequent laser pulses at all laser wavelengths used. In addition, at higher fluence and number of pulses broad bands assigned to the D and G bands are seen. XPS investigations displayed clearly distinct chemical changes in the trenches only in one case: sample treated by NIR irradiation 1064 nm 66 pulses. These changes identify occurrence of silicon oxidation in different degrees and presence of some quantities of OH group. In this case a possible influence of the number of the pulses is observed: an increase of oxidation degree at their higher number.

#### Acknowledgements

Financial support of the State Fond “Scientific Research”, Bulgaria for the project T02/24 is acknowledged. Parts of this work are made within the frame of bi-lateral projects for collaboration between Bulgarian Academy of Sciences (BAS) and FWO (Fonds Wetenschappelijk Onderzoek, Belgium). The authors thank Prof. T. Vladkova for her assistance in supplying the PDMS.

#### References

- [1] A.C.M. Kuo, in: J.E. Mark (Ed.), *Polymer Data Handbook*, Oxford University Press, London, 1999. <http://www.toarplast.co.il/linkspage/handbook.pdf>.
- [2] J.C. Caprino, R.F. Macander, in: M. Morton (Ed.), *Rubber Technology*, Springer Science + Business Media Dordrecht, Berlin, Heidelberg, Germany, 1999.
- [3] Y. Qina, M.M.R. Howlader, M.J. Deena, Y.M. Haddara, P.R. Selvaganapathy, Polymer integration for packaging of implantable sensors, *Sens. Actuators B* 202 (2014) 758–778.
- [4] J.C. McDonald, D.C. Duffy, J.R. Anderson, D.T. Chiu, H. Wu, O.J.A. Schueller, G.M. Whitesides, Fabrication of microfluidic systems in poly(dimethylsiloxane), *Electrophoresis* 21 (2000) 27–40.
- [5] T.G. Vladkova, I.L. Keranov, P.D. Dineff, S.Y. Youroukov, I.A. Avramova, N. Krasteva, G.P. Altankov, Plasma based  $Ar^+$  beam assisted poly(dimethylsiloxane) surface modification, *Nuclear Instrum. Methods Phys. Res. B* 236 (2005) 552–562.
- [6] H. Hillborg, J.F. Ankner, U.W. Gedde, G.D. Smith, H.K. Yasuda, K. Wikstrom, Crosslinked poly(dimethylsiloxane) exposed to oxygen plasma studied by neutron reflectometry and other surface specific techniques, *Polymer* 41 (2000) 6851–6863.
- [7] C. Donzel, M. Geissler, A. Bernard, H. Wolf, B. Michel, J. Hilborn, E. Delamar, Hydrophilic poly(dimethylsiloxane) ptamps for picrocontact printing, *Adv. Mater.* 13 (2001) 1164–1167.
- [8] L. Urech, T. Lippert, in: C. Phipps (Ed.), *Laser Ablation and its Applications*, Springer, Berlin, Heidelberg, Germany, 2007.
- [9] V.-M. Graubner, O. Nuyken, T. Lippert, A. Wokaun, S. Lazare, L. Servant, Local chemical transformations in poly(dimethylsiloxane) by irradiation with 248 and 266 nm, *Appl. Surf. Sci.* 252 (2006) 4781–4785.
- [10] C. Dupas-Bruzek, O. Robbe, A. Addad, S. Turrell, D. Derozier, Transformation of medical grade silicone rubber under Nd:YAG and excimer, laser irradiation: first step towards a new miniaturized nerve electrode fabrication process, *Appl. Surf. Sci.* 255 (2009) 8715–8721.
- [11] L.D. Laude, K. Kolev, C. Dicara, C. Dupas-Bruzek, Laser metallization for microelectronics and bio-applications, *Proc. SPIE* 4977 (2003) 578–586.
- [12] L.D. Laude, C. Cochrane, C. Dicara, C. Dupas-Bruzek, K. Kolev, Excimer laser decomposition of silicone, *Nuclear Instrum. Methods Phys. Res. B* 208 (2003) 314–319.
- [13] C. Dicara, T. Robert, K. Kolev, C. Dupas-Bruzek, L.D. Laude, Excimer laser processing of silicone rubber: from understanding the process to applications, *Proc. SPIE* 5147 (2003) 255–265.
- [14] P.A. Atanasov, N.N. Nedyalkov, E.I. Valova, Z.S. Georgieva, S.A. Armyanov, K.N. Kolev, S. Amoroso, X. Wang, R. Bruzzese, M.W. Sawczak, G. Iiwiski, Fs-laser processing of polydimethylsiloxane, *J. Appl. Phys.* 116 (2014) 023104.
- [15] N.E. Stankova, P.A. Atanasov, N.N. Nedyalkov, T.R. Stoyanchov, K.N. Kolev, E.I. Valova, J.S. Georgieva, S.A. Armyanov, S. Amoroso, X. Wang, R. Bruzzese, K. Grochowska, G. Sliwinski, K. Baert, A. Hubin, M.P. Delplancke, J. Dille, Fs- and Ns-laser processing of polydimethylsiloxane (PDMS) elastomer: comparative study, *Appl. Surf. Sci.* 336 (2015) 321–328.
- [16] C. Palma, M.C. Rossi, C. Sapia, E. Bemporad, Laser-induced crystallization of amorphous silicon-carbon alloys studied by Raman microscopy, *Appl. Surf. Sci.* 138–139 (1999) 24–28.
- [17] B. Schnyder, T. Lippert, R. Koetz, A. Wokaun, V.-M. Graubner, O. Nuyken, UV-irradiation induced modification of PDMS films investigated by XPS and spectroscopic ellipsometry, *Surf. Sci.* 532–535 (2003) 1067–1071.
- [18] H. Hillborg, J.F. Ankner, U.W. Gedde, G.D. Smith, H.K. Yasuda, K. Wikström, Crosslinked polydimethylsiloxane exposed to oxygen plasma studied by neutron reflectometry and other surface specific techniques, *Polymer* 41 (2000) 6851–6863.
- [19] H. Hillborg, U.W. Gedde, Hydrophobicity recovery of polydimethylsiloxane after exposure to corona discharges, *Polymer* 39 (1998) 1991–1998.
- [20] V.-M. Graubner, R. Jordan, O. Nuyken, B. Schnyder, T. Lippert, R. Koetz, A. Wokaun, Photochemical modification of cross-linked poly(dimethylsiloxane) by irradiation at 172 nm, *Macromolecules* 37 (2004) 5936–5943.
- [21] T. Lippert, Interaction of photons with polymers: from surface modification to ablation, *Plasma Process Polym.* 2 (2005) 525–546.
- [22] M.A. Kelly, in: D. Briggs, J.T. Grant (Eds.), *Surface Analysis by Auger and X-ray Photoelectron Spectroscopy*, IM Publications, Chichester, UK, 2003.
- [23] S. Hofmann, Auger- and X-ray Photoelectron Spectroscopy in Materials Science. A User-Oriented Guide, Springer-Verlag, Berlin, Heidelberg, 2013.
- [24] G. Beamson, D. Briggs (Eds.), *The XPS of Polymers Database*, Surface Spectra Ltd., Manchester, UK, 2012, ISBN 0-9537848-4-3.
- [25] P. Louette, F. Bodino, J.-J. Pireaux, Poly(dimethyl siloxane) (PDMS) XPS reference core level and energy loss spectra, *Surf. Sci. Spectra* 12 (2005) 38–43.
- [26] J. O'Connor, in: K. Wandelt (Ed.), *Surface and Interface Science*, Volumes 1 and 2, Wiley VCH, Weinheim, Germany, 2012.
- [27] S. Hofmann, Auger- and X-Ray Photoelectron Spectroscopy in Materials Science. A User-Oriented Guide, Springer-Verlag, Berlin Heidelberg, Germany, 2013.
- [28] M.P. Seah, in: D. Briggs, J.T. Grant (Eds.), *Surface Analysis by Auger and X-ray Photoelectron Spectroscopy*, IM Publications, Chichester, UK, 2003.
- [29] M.R. Alexander, R.D. Short, F.R. Jones, W. Michaeli, C.J. Blomfield, A study of HMDSO/O plasma deposits using a high-sensitivity and -energy resolution XPS instrument: curve fitting of the Si 2p core level, *Appl. Surf. Sci.* 137 (1999) 179–183.
- [30] L.-A. O'Hare, B. Parbhoo, S.R. Leadley, Development of a methodology for XPS curve-fitting of the Si 2p core level of siloxane materials, *Surf. Interface Anal.* 36 (2004) 1427–1434.
- [31] Wagner CD, Riggs WM, Davis LE, Moulder JF, Muilenberg GE (ed.), *Handbook of X-Ray Photoelectron Spectroscopy, A Reference Book of Standard Data For Use In X-Ray Photoelectron Spectroscopy*. Perkin-Elmer Corporation Physical Electronics Division 6509 Flying Cloud Drive Eden Prairie, Minnesota, USA, 1979.
- [32] A.U. Alam, M.M.R. Howlader, M.J. Deen, Oxygen plasma and humidity dependent surface analysis of silicon, silicon dioxide and glass for direct wafer bonding, *J. Solid State Sci. Technol.* 2 (2013) P515–P523.
- [33] J.R. Pitts, T.M. Thomas, A.W. Czanderna, M. Passler, XPS and ISS of submonolayer coverage of Ag on SiO<sub>2</sub>, *Appl. Surf. Sci.* 26 (1986) 107–120.
- [34] S.S. Chao, Y. Takagi, G. Lucovsky, P. Pai, R.C. Custer, J.E. Tyler, J.E. Keem, Chemical states study of Si in SiO<sub>x</sub> films grown by PECVD, *Appl. Surf. Sci.* 26 (1986) 575–583.
- [35] J. Finster, E.-D. Klinkenberg, J. Heeg, ESCA and SEXAFS investigations of insulating materials for ULSI microelectronics, *Vacuum* 41 (1990) 1586–1589.